ELSEVIER

Ceramics International 31 (2005) 953–958

CERAMICS INTERNATIONAL

www.elsevier.com/locate/ceramint

Synthesis, evaluation and characterization of alumina ceramics with elongated grains

Lihua Xu [a,*], Zhipeng Xie [b], Lichun Gao [a], Xidong Wang [a], Fang Lian [a], Tong Liu [b], Wenchao Li [a]

[a] *Department of Inorganic Materials, University of Science and Technology Beijing, Beijing 100083, PR China*
[b] *State Key Laboratory of New Ceramic and Fine Process, Tsinghua University, Beijing 100084, PR China*

Received 30 July 2004; received in revised form 9 September 2004; accepted 10 October 2004
Available online 25 February 2005

Abstract

Alumina ceramics with high fracture toughness were synthesised by introducing seeds and controlling processing using the in situ self-toughening technique. The preparation of the high tough alumina materials started with cheap commercial aluminum hydroxide as raw materials. α-Alumina powder was gained by low temperature calcination of the aluminum hydroxide with seeds, which were introduced by high purity alumina ball medium during grinding. The alumina powders were hot-pressed, then, the high tough alumina ceramics with elongated grains were obtained. The elongated grain structure is originally considered to play a significant role in the increment of fracture toughness. Meanwhile, in order to investigate in situ toughening mechanism of elongated alumina grains, which can produce crack bridging, crack deflection and pull-out as dominant toughening mechanisms to greatly increase toughness, fractal characteristics and model were studied in detail.

Keywords: D. Alumina; Elongated grain; Fracture toughness; Fractal characteristics

1. Introduction

It is known that fracture toughness of ceramics such as Si_3N_4–SiC (w) is enhanced by the presence of elongated grains or second phases in the microstructure, promoting crack deflection and crack bridging [1]. The microstructure can be achieved by a simple strategy, i.e., dispersing a suitable second phase in matrix. For example, platelets, whisker, fiber, or transformable particles can be incorporated into the matrix [2–4]. As a result, whisker-reinforced composites appear to have some of the best properties, but health hazards associated with handling whiskers have significantly curtailed industrial acceptance and implementation. Continuous fiber reinforced composites have been used in only limited applications due to the relatively high cost of manufacture. On the other hand, these improvements in toughness of composites may occur at the expense of strength, while the second phase acts as a flaw initiation site. It is well recognized that second phases may also inhibit densification, making it necessary to hot press or HIP to gain high densities. This may be attributed to the constraint of the second phase network.

In situ formation of a second phase with a highly anisotropic growth habit can be designed for a high toughness ceramic composite without the sintering difficulty. Hori et al. reported about an in situ composite of TiO_2 matrix with dispersed corundum platelets whose anisotropic growth was promoted by sodium doping. A toughness of up to 7 MPa $m^{1/2}$ was attained [5]. Alumina composites containing in situ formed four kinds of hexaluminate ($LaAl_{11}O_{18}$, $LaMgAl_{11}O_{19}$, $SrAl_{12}O_{19}$ and $Mg_2NaAl_{15}O_{25}$) platelets can be fabricated even by pressureless sintering process to attain high density, and a peak toughness 50% higher than that of alumina is obtained at the sample containing 30 vol% of aluminates [6]. Masaki et al. [7]

* Corresponding author. Fax: +86 10 6232 7283.
E-mail address: xulihua1966@263.net (L. Xu).

0272-8842/$30.00
doi:10.1016/j.ceramint.2004.10.008

reported that elongated alumina grains in the Al_2O_3/$LaAl_{11}O_{18}$ system were formed by doping with small addition of silica, on the order of several hundred ppm, subsequent 20 vol% lanthana-alumina was in situ formed. Its strength of over 600 MPa and high toughness (6 MPa $m^{1/2}$) were achieved. Similar results were found in Al_2O_3 matrix composites by in situ reaction in the Al_2O_3–La_2O_3 system [8], and in TiO_2-doped alumina with anisotropic grain growth [9].

In research work parallel to the present one, we have developed a promising and useful process for elongated alumina grains using homogeneous seeds incorporated into matrix [10–12], instead of heterogeneous expensive additives, such as titania or lanthana. The emphasis on the present work is to demonstrate systematically the relationships among fractal characteristics, microstructure and mechanical properties. How to prepare these self-toughening alumina ceramics with elongated grains is referred in detail.

2. Experimental procedure

Commercially available high-purity aluminum hydroxide with a mean particle size of 2.84 μm (purity > 98%, in the presence of impurities such as Na_2O, MgO, SiO_2 and CaO, Wenzhou Alum Institute, China), which was synthesized by Bayer process, was used as starting material. Alumina milling ball, as a seed source into aluminum hydroxide during grinding, was made of high-purity α-alumina with a mean particle size of 0.3–0.4 μm (purity > 99%, Ceralox, USA). For a comparative study of the effect of seed-doped on anisotropic grain growth and microstructure of alumina ceramics, it was necessary to fabricate traditionally alumina without seed additive as a reference specimen. Thus, α-alumina industrial powder with a mean particle size of 2.9 μm (purity > 97%, Henan Xinyuan Co. Ltd., China) was also used, as tabularized in Table 1.

Aluminum hydroxide powders and alumina balls were mixed by planetary milling for 72 h using distilled water at a powder-to-ball-to-water ratio of about 1:15:6. The seed weight fraction can also be characterized. The as milled aluminum hydroxide powders were air-dried at 80 °C for 30 h on heating oven. The calcination test in box furnace at air was performed for these powders. They were initially heated to 1100 °C at a rate of 5 °C/min, and then were maintained at this temperature for 2 h, a natural cooling followed by switching off the power. Therefore, ultrafine α-alumina powders with a mean particle size of 0.85 μm, were gained at low temperature calcination while the initial particles experienced a decomposing and phase-transforming process that could be determined by TG and DTA analysis [13,14]. The cylindrical pellet of as-heated treatment powders was uniaxially die-pressed at 100 MPa, placed on a graphite crucible followed by HP sintering under argon atmosphere. They were first fired to 1100 °C, and initially brought pressure to bear on the compact. While the temperature up to 1600 °C, it was kept for a required time under the controlling of pressure of 40 MPa. Finally, the cooling rate was 5 °C/min.

Table 1
Specifications of raw Al_2O_3 powder

Purity Al_2O_3 (wt.%)	99.7
SiO_2 (wt.%)	0.05
Fe_2O_3 (wt.%)	0.03
Na_2O (wt.%)	0.05
B_2O_3 (wt.%)	0.04
L.O.I. (wt.%)	0.1
Crystalline phase	α-alumina (>95 wt.%)
Density (g/cm^3)	>3.96

Bulk density was measured by the Archimedes method. X-ray diffraction analysis (XRD, RAD-RB, Rigaku Ltd., Japan) was conducted for phase identification using Cu Kα radiation (40 kV, 100 mA). Microstructure and crack propagation behavior observations using electron microscopy (SEM, S-450, Hitachi Co., Japan) were made on polished and fractured surfaces. Test pieces for bending strength measurement (3 mm × 4 mm×36 mm) and for fracture toughness measurement (4 mm × 6 mm × 30 mm) were respectively sliced from sintered plates using diamond wheel toward the vertical tensile axis of bend bars. Each surface of a bar was ground on plane grinding machine (M7120D, Tianjin, China), and polished by hand using seven polishing paste in series of $28^{\#}$, $14^{\#}$, $7^{\#}$, $5^{\#}$, $3.5^{\#}$, $2.5^{\#}$ and $1^{\#}$. Three-point flexural strength test was carried out with a span of 30 mm, and a crosshead speed of 0.5 mm/min at room temperature. Fracture toughness was determined by the single-edge-precracked beam (SEPB) method with a span of 24 mm, and the length of the precracks for all specimens was from 1.9 to 2.5 mm.

3. Results and discussion

3.1. Microstructure and mechanical property of alumina ceramics with elongated grain

Fig. 1 shows SEM micrographs of polished and thermal etched surface of conventional alumina (no seed source) and seed-doped alumina, respectively. The grains in the monophase alumina sintered at 1600 °C, are traditionally equiaxed as illustrated in Fig. 1(A) and the mean grain size was about 6 μm. Fig. 1(B) presents that the material contains a large scale in situ formed alumina with elongated grain, initially induced by needle-shaped alumina seed. The different structures between equiaxial grain and anisotropic grain make them readily distinguishable in electron micrographs.

The size and shape of these elongated grains are similar. Its mean grain length can be measured, of 5 μm, and the length-to-diameter ratio is about 7:1. It implies that a dependence of seed additive on formation of elongated grain

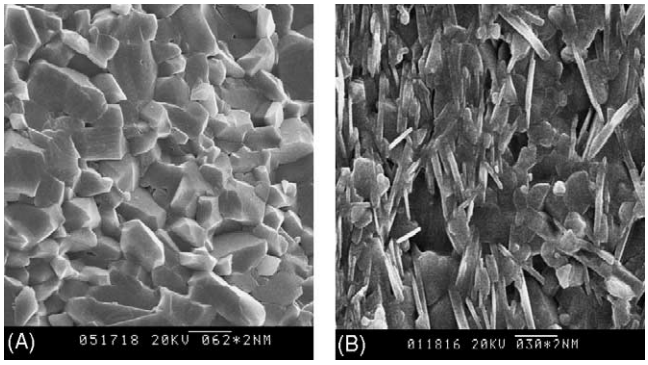

Fig. 1. Microstructures observed in (A) monolithic alumina sintered at 1600 °C for 2 h, and (B) seed-doped alumina sintered at 1600 °C for 2 h.

under the condition of HP sintering is quite effective and strong. Monolithic alumina exhibited a relatively low fracture toughness of only 4.0 MPa $m^{1/2}$. However, the elongated alumina displayed a higher toughness (i.e., exceeding 7 MPa $m^{1/2}$) with an increment of over 75% if compared with the toughness of monolithic alumina. The result is in agreement with or even better than that reported in existing literatures [5–9]. It might be attributed to the elongated effect by consubstantial seeds in accordance with alumina matrix.

On the other hand, it is known in later case for the grains to grow in situ only in specific directions. Also, it is difficult to attain an in situ identical orientating due to disordered distribution of original particles, and the resultant toughening contribution is smaller.

The bending strength is plotted in Fig. 2 as a function of holding time at high temperature. Interestingly, the strength remains constant of about 400 MPa in seed-doped specimens sintered at 1600 °C even within the holding-time range of 0.5–1 h. Nevertheless, a peak strength 40% higher than that only maintaining 1 h can be seen as increasing the time up to 2 h. Furthermore, the specimen has the same maximum toughness compared with the others. The slight reduction in strength as time of 4 h could be attributed to formation of defects in the presence of coarser grain with abnormal grain growth.

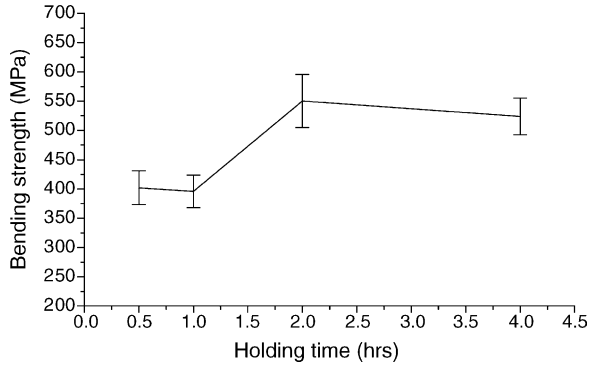

Fig. 2. The bending strength of in situ growth alumina sintered at 1600 °C within holding time range of 0.5–4 h.

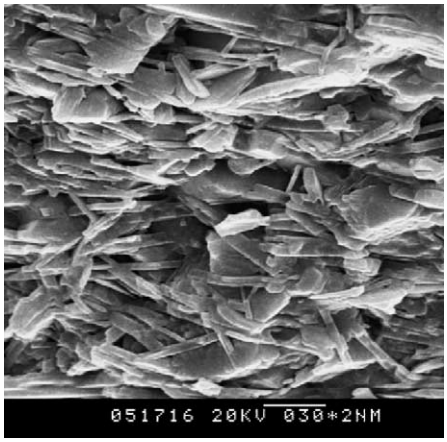

Fig. 3. Scanning electron micrograph of fractured surface of self-toughening alumina with anisotropic grain structure.

3.2. Fractal characteristic and mechanical model of alumina ceramics with several typical structures through various process

Fig. 3 shows micrograph observed in the fractured surface of in situ growth alumina specimen. It reveals a combined characteristic involving transgranular fracture and intergranular fracture. The result support our view of self-toughening mechanism which can produce crack bridging, crack deflection and pull-out to greatly increase both fracture toughness and bending strength, suggesting an increment in toughness is proportional to elongated grain size of the material.

To elucidate the influence of microstructural feature including grain shape, size and distribution, etc., responsible for the increment in toughness, it is necessary to establish a relevant fractal model on the principle of fractal geometry where the geometrically irregular surfaces (metal, carbon, rock, etc.) could be quantificationally described [15,16]. In the high performance ceramics toughened by second phase, the combined action of crack deflection and crack bridging takes place with a significant increase in fracture toughness [3]. Considering these factors, the fractal characteristic in fracturing process can be determined involving how crack propagation along grain boundary (intergranular fracture) or through grain interior (transgranular fracture).

3.2.1. Diagram explanatory for crack propagation path

Assuming the obtaining of equiaxial hexangular alumina grains with normal growth in the case of full densification (as shown in Fig. 1), the grain arrangement in closed packing way, can schematically be presented in Fig. 4(A) and (B). Due to intergranular fracture behaving as a dominant toughening mechanism followed by crack propagation towards grain boundary of monolithic ceramic, the alternative crack extending path is shown in Fig. 4(A) and (B). Meanwhile, Fig. 4(C) illustrates crack extending path in alumina with different grain size originating from abnormal growth, for example it sintering at extremely high

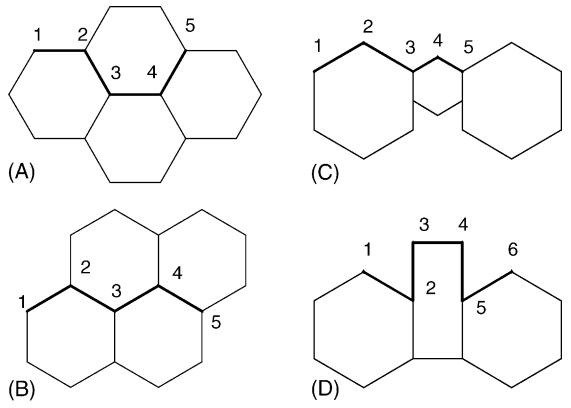

Fig. 4. Crack propagation of several typical alumina ceramics. A, B: monolithic alumina ceramics with normal grain growth, C: monolithic alumina ceramics with abnormal grain growth, and D: alumina ceramics with reinforcement of elongated grains.

temperature or for long time. For in situ formed alumina with elongated grain, the crack propagation path is hypothetically shown in Fig. 4(D), where transgranular fracture simultaneously appears in the process of 3–4. Such phenomena are also observed in Fig. 3.

3.2.2. Fundamentals of fractal geometry

Based on the fractal geometry deduced by Mandelbrot, the fractal dimension, d_f, critical linear crack propagation forces, G_{crit} and microscopic fracture toughness, K_{IC}^{Micro} can be expressed in the following equations, respectively [17].

$$d_f = \frac{\log(N)}{\log(1/r)} \tag{1}$$

where N is numbers in fractal curve using various scaled lengths, r is ratio of similarity.

$$G_{crit} \approx 2\gamma_s D^{(1-d_f)} = 2\gamma_s \left(\frac{1}{r}\right)^{(d_f-1)} \tag{2}$$

where γ_s is interfacial energy of ceramics, D is grain size, can be defined as $1/r$.

However, classical fracture theory simply regards crack propagation path as a line, i.e., $d_f = 1$, $G_{crit} = 2\gamma_s$, so, the macroscopic fracture toughness is merely formulated as:

$$K_{IC}^{Macro} = (EG_{crit})^{1/2} = (2E\gamma_s)^{1/2} \tag{3}$$

where E is an elastic modulus of ceramics. Factually, if fractal feature considered, crack propagation experiences as an irregular route (in zigzag way). Therefore, a complete expression for microscopic fracture toughness is demonstrated as:

$$K_{IC}^{Micro} = (EG_{crit})^{1/2} = (2E\gamma_s)^{1/2}(1/r)^{(d_f-1)/2} \tag{4}$$

3.2.3. Derivation of fractal characteristic and mechanical models in alumina ceramics

(I) In the case of monolithic alumina with normal grain growth, the physical parameters can be given according to above Eqs. (1)–(4).

$$N = 4, \quad r = \frac{1}{3}, \quad d_f = \frac{\log 4}{\log 3} = 1.26 \quad \text{(Fig. 5A)}$$

$$N = 2, \quad r = 3^{-0.5}, \quad d_f = 2\frac{\log 2}{\log 3} = 1.26 \quad \text{(Fig. 5B)}$$

$$G_{crit}^{A} = 3^{0.26} \times 2\gamma_s = 1.33 \times 2\gamma_s;$$

$$G_{crit}^{B} = 1.732^{0.26} \times 2\gamma_s = 1.15 \times 2\gamma_s$$

$$K_{IC}^{Micro,A} = 1.15 \times (2E\gamma_s)^{1/2};$$

$$K_{IC}^{Micro,B} = 1.07 \times (2E\gamma_s)^{1/2}$$

Under the two circumstances, the same fractal dimension d_f in (A) as that in (B) can be found. In comparison with that in (A), the as obtained G_{crit}^{B} value appears to so small that there is an easily occurred path of crack propagation in the case of (B), and its microscopic fracture toughness is also small.

(II) In the case of monolithic alumina with abnormal grain growth, assuming that edge length of large grain (the length of 1–2 as shown in Fig. 5(C)) is 1 as a unit length, and that of small grain is q ($0 < q < 1$). The parameters are given as follows:

$$N = 2(1+q), \quad r = 3^{-1/2}(1+q)^{-1},$$
$$d_f = \frac{\log[2(1+q)]}{\log[3^{1/2}(1+q)]}$$

In accordance with Eqs. (2) and (4), the G_{crit} and K_{IC}^{Micro} can be calculated on the basis of the as given d_f and r:

$$G_{crit} = 2\gamma_s \left(\frac{1}{r}\right)^{(d_f-1)}$$
$$= 2\gamma_s [3^{1/2}(1+q)]^{\left\{\frac{\log[2(1+q)]}{\log[3^{1/2}(1+q)]}-1\right\}}$$
$$= 2\gamma_s [3^{1/2}(1+q)]^{\left\{\frac{\log(2/3^{1/2})}{\log[3^{1/2}(1+q)]}\right\}}$$

Logarithm is taken for both left and right in upper equation. Hence, the complex equation would be simplified as follows:

$$\log G_{crit} = \log(2\gamma_s) + \log[3^{1/2}(1+q)] \times \frac{\log(2/3^{1/2})}{\log[3^{1/2}(1+q)]} = \log(2\gamma_s) + \log(2/3^{1/2})$$

$$\therefore \quad G_{crit} = 2 \times 3^{-1/2} \times 2\gamma_s = 1.15 \times 2\gamma_s$$

$$K_{IC}^{Micro} = (EG_{crit})^{1/2} = 1.07(2E\gamma_s)^{1/2}$$

From the above results, it is not difficult to find that both the G_{crit} and the K_{IC}^{Micro} in (C) are surprisingly equal to the relevant values in (B). Whereas, the changeable d_f in (C), within the value range of 1.12–1.26 ($0 < q < 1$), differs from the constant (1.26) in (B) or (A). The great discovery might successfully

Table 2
Comparisons of experimental results (K_{IC}^{Test}) with several predictions (K_{IC}^{Macro}, K_{IC}^{Micro}) using classical fracture theory and the present models

Materials	Alumina with equiaxed grain	Alumina with elongated grain
K_{IC}^{Test} (MPa m$^{1/2}$)	4.0	7.1
γ_s (J/m^2)	18	32 (γ_{ss})
E (GPa)	380	380
K_{IC}^{Macro} in Eq. (3)	3.70	4.93
Deviation[a] (%)	7.5	30.6
K_{IC}^{Micro} in fractal models	3.96 Model (I) (case of B)	6.66 Model (III)
Deviation[b] (%)	1.0	6.2

[a] $\left|\frac{K_{IC}^{Test}-K_{IC}^{Macro}}{K_{IC}^{Test}}\right|$.
[b] $\left|\frac{K_{IC}^{Test}-K_{IC}^{Micro}}{K_{IC}^{Test}}\right|$.

interpret why non-toughening effect yields in ceramic matrix composites (CMC) using spherical or cubical particles while different size as dispersing agents, except incorporated with rod-like or whisker with a large ratio of length-to-diameter [18,19].

(III) In the case of self-toughening alumina with elongated grain, fractal unit of fracture is illustrated as Fig. 5(D) (from 1 to 6). The parameters are given in the following expressions:

$$N = 5, \quad r = \frac{1}{(1+3^{1/2})}, \quad d_f = \frac{\log 5}{\log(1+3^{1/2})} = 1.60$$

$$G_{crit} = 2.732^{0.60} \times 2\gamma_{ss} = 1.83 \times 2\gamma_{ss},$$

$$K_{IC}^{Micro} = (EG_{crit})^{1/2} = 1.35(2E\gamma_{ss})^{1/2}$$

Here, γ_{ss} value is greater than γ_s in the case of (I) and (II) owing to a difference between grain interior (46 J/m^2) and grain boundary (18 J/m^2) [20]. If an equal extent contributed by transgranular and intergranular is presumed, $\gamma_{ss} \approx 32$ J/m^2.

Alumina ceramics, subjected to various fabricating routes, exhibit a great dissimilar microstructure and mechanical properties. As all these auxiliary physical properties including E, γ_s and γ_{ss} are determined (or estimated), the fracture toughness may be evaluated in accordance with the existing classical model, derivative models (I) and (III), as well as the as-tested value intercepted (seeing Fig. 2), are comparatively listed in Table 2.

It can been seen that there is a big error of 7.5% in the evaluation using classical theory for fracture toughness of alumina with equiaxed grain, than that (only 1%) using presenting fractal model (I) in the B case. Also, the huge deviation of 30.6% is given as the estimation of K_{IC}^{Macro} in adopting Eq. (3). It indicates that the classical is bad in agreement with prediction for the self-toughening ceramics. In contrast, the presented model (III) displays accuracy that the deviation is only 6.2%, while evaluating in alumina ceramics/refractories toughened by elongated grain.

4. Summary

Instead of expensive additives of lanthana, the introduction of seeds into alumina matrix is another novel approach to obtain in situ growth of elongated grain, which can improve greatly mechanical properties. Thus, higher toughness can reach to 7.1 MPa m$^{1/2}$, in agreement with or even better than that reported in existing refs [5–9], in comparison with conventional alumina ceramics/refractories (4 MPa m$^{1/2}$). The difference of structures between equiaxial grain and elongated grain makes them readily distinguishable in electron micrographs. These in situ formed grains have a uniform orientation and a similar size and shape, where the mean grain length is 5 μm, and the length-to-diameter ratio is about 7:1. The formation and development of elongated structure is sensitive to the holding time followed by hot press sintering. As the specimen sintering at 1600 °C for 2 h, peak strength 40% higher than that only maintaining 1 h can be attained.

To demonstrate relationships between toughness and specific microstructure, the fractal characteristic and mechanical model have been put forward in accordance with crack propagation path and crack deflection extent. On the principle of fractal geometry, fractal dimension, critical linear crack propagation forces and microscopic fracture toughness are respectively calculated in the following cases, i.e., monolithic alumina with normal grain growth, monolithic alumina with abnormal grain growth, and self-toughening alumina with elongated grain. The presented fractal models (I and III) exhibit a reasonable accuracy in predicting microscopic fracture toughness in which there is a small deviation (1 and 6.2%) for alumina with equiaxed grain and with elongated grain, respectively. However, if using classical fracture theory, a large error appears to exist whose value is 7.5 and 30.6% in above materials. In addition, the model (II) with the same theoretical toughness as model in the case of B is derived from equiaxed grains originating from abnormal growth or introducing of second phase. It can successfully explain the fact that there are never any contributions to toughness of ceramic composites with reinforcement of spherical particles.

Acknowledgements

This work was supported by the Natural Science Foundation of China (Grant No. 50332010, 50172022, 50172008), High-tech R&D 863 Project (No. 2002AA334080), Education Committee Return Overseas Scholars and Key Sci & Tech Program (No. 03020), Funding of State Laboratory of New Ceramics and Fine Processing of Tsinghua University (X.GZ0209), and also by the Foundation for Sci & Tech of Portugal (PRAXISXXI/BPD/22082/99).

Appendix A

The term "Fractal" was coined from the Latin adjective fractus. Fractal geometry was introduced by B.B. Mandelbrot [15]. For D-dimension standard shapes such as a rectangle, when it follows for every side "base" b that "whole" make up of the shape can be "paved" exactly by $N = b^D$ parts, each part can be deduced from the whole by a similarity of ratio

$$r(d) = \frac{1}{N^{1/d}}$$

Equivalent alternative expression is written by

$$d = \frac{\log(N)}{\log(1/r)}$$

For non-standard sharp, in order for the similarity of ratio to have the same form as the above, the sole requirement is for the shape to be self-similar. The D obtained in this fashion is called the self-similarity dimension. A fractal set is a set for which Hausdorff Besicovitch dimension d strictly exceeds the topological dimension d_T. A fractal often has self-similarity or statistically self-similarity (known as linearly fractal), therefore its dimension can be estimated according to the self-similarity dimension. When the length $L(\varepsilon)$ of a fractal curve is measured with the yardstick length ε, then, according to Mandelbrot's results [16]:

$$L(\varepsilon) = \varepsilon^{1-d_f}$$

where d_f denotes the fractal dimension. In a brittle material, linear crack propagation forces G_{crit} can be characterized based on fractal theory [16]:

$$G_{crit} \approx 2\gamma_s D^{(1-d_f)}$$

where γ_s is interface energy of materials, D is grain size.

References

[1] P.F. Becher, Microstructural design of toughed ceramics, J. Am. Ceram. Soc. 74 (1991) 255–269.
[2] Y. Jiandong, W. Jianqing, W. Yingjun, L. Hongyan, Fabrication, microstructure and mechanical properties of in situ Al_2O_3 platelets reinforced Ce-TZP composites, Key Eng. Mater. 224–226 (2002) 341–346.
[3] H. Yoshihiro, M. Shinichi, I. Yoshimi, Colloidal processing and mechanical properties of whisker-reinforced mullite matrix composites, J. Am. Ceram. Soc. 74 (1991) 2438–2442.
[4] L.H. Xu, Z.P. Xie, J.B. Li, Y. Huang, X.D. Fan, H.W. Xu, Microwave annealing of yttria stabilized zirconia ceramics, J. Mater. Sci. Lett. 16 (1997) 1249–1251.
[5] S. Hori, H. Kaji, M. Yoshimura, S. Somiya, Deflection toughened corundum rutile composition, Mater. Res. Soc. Symp. Proc. 78 (1987) 283–288.
[6] C. Pei-Lin, C.I. Wei, In-situ alumina/aluminate platelet composites, J. Am. Ceram. Soc. 75 (1992) 2610–2612.
[7] Y. Masaki, H. Kiyoshi, E.B. Manuel, K. Shuzo, High-strength and high fracture toughness ceramics in $Al_2O_3/LaAl_{11}O_{18}$ system, J. Am. Ceram. Soc. 78 (1995) 1853–1856.
[8] K.J. Byung, K. Teruo, Fabrication and microstructure of Al_2O_3 matrix composites by in-situ reaction in the Al_2O_3–La_2O_3 system, J. Ceram. Soc. Jpn. 106 (1998) 739–743.
[9] S.H. Debra, L.M. Gary, Anisotropic grains growth in TiO_2-doped alumina, Mater Sci. Eng. A195 (1995) 169–178.
[10] Z.P. Xie, J.W. Lu, L.C. Gao, W.C. Li, L.H. Xu, Influence of different seeds on transformation of aluminum hydroxides and morphology of alumina grains by hot pressing, Mater. Des. 24 (2003) 209–214.
[11] L.C. Gao, L.H. Xu, Z.P. Xie, Novel preparing route for self toughening alumina ceramic materials, J. Chin. Rare Earth Soc. 20 (2002) 518–524.
[12] Z.P. Xie, L.C. Gao, W.C. Li, L.H. Xu, X.D. Wang, High toughness alumina ceramics with elongated grains developed from seeds, Sci. Chin. 46 (2003) 527–536.
[13] L. Tong, The Preparation of High Fracture Toughness Alumina with Elongated Grains. Master Dissertation, Tsinghua University, Beijing, 2001.
[14] Z.P. Xie, T. Liu, Y. Huang, Y.B. Cheng, Fracture toughness improvement of alumina with elongated grains, J. Aust. Ceram. Soc. 36 (2000) 97–102.
[15] B.B. Mandelbrot, D.E. Passoja, Fractal character of fracture surface of metals, Nature 308 (1984) 721–724.
[16] B.B. Mandelbrot, The Fractal Geometry of Nature, Freeman (Ed.), San Francisco, 1982, p. 1.
[17] L.H. Xu, Y. Huang, H. Guo, Z.S. Ding, Progress on fractal characteristic in fracture behavior of solid materials, J. Chin. Ceram. Soc. 25 (1997) 458–463.
[18] X.D. Wang, S.C. Du, W.C. Li, Kinetic studies of oxidation of γ-aluminum oxynitride, Metall. Mater. Trans. B 33 (2002) 201–207.
[19] L.H. Xu, G.Q. Nie, F. Lian, Investigation of the preparing process and mechanical properties of alumina-mullite refractory with reinforcement of SiAlON, Key Eng. Mater. 224–226 (2002) 287–290.
[20] Z.D. Guan, Physical Properties of Inorganic Material, Tsinghua University Press, Beijing, 1992, pp. 232–252.